Antibody Binding to Lipid Model Membranes. The Large-Ligand Effect†

Lukas K. Tamm* and Ingrid Bartoldus
Department of Biophysical Chemistry, Biocenter, University of Basel, CH-4056 Basel, Switzerland
Received February 17, 1988; Revised Manuscript Received May 24, 1988

ABSTRACT: A method, based on resonance energy transfer, has been developed to measure the binding of fluorescein-labeled, monoclonal anti-lipid hapten antibodies to rhodamine B labeled liposomes. The binding of this antibody was studied as a function of the trinitrophenol–lipid hapten density in unilamellar phosphatidylcholine vesicles. Although the experimental data at a given lipid hapten density could be fit successfully to conventional Langmuir-type binding isotherms (or the corresponding Scatchard plots), this treatment leads to inconsistent binding constants and lipid hapten to antibody stoichiometries. However, our binding data could be described successfully with a statistical binding model, which included effects due to steric hindrance of the large ligands [Stankowski, S. (1983) *Biochim. Biophys. Acta 735*, 352–360] and which was adapted to the problem of bivalent antibody binding to small mobile binding sites in a fluid membrane. All experimental binding isotherms in the range of 0.1–5 mol % lipid hapten are easily simulated with this model by using only a single binding constant of 2.8×10^{10} M^{-1} and the given lipid hapten density. The large-ligand effect, demonstrated here in the antibody–lipid hapten system, may also have profound consequences in many other biologically important cases.

The binding of large, macromolecular ligands to smaller receptors in membranes is widespread in immunology and general membrane biology. For example, the Wasserman antibodies (IgM) bind to cardiolipin in syphilis patients (Pangborn, 1942); anti-lipid antibodies with various lipid headgroup specificities are also rather ubiquitous in most normal sera (Alving, 1984); the first subcomponent of complement (C1q) recognizes several surface-bound antibodies before further components bind and the whole complement cascade is triggered (Schumaker et al., 1987); an alternative activation of C1q by cardiolipin in model membranes has also been reported (Peitsch et al., 1987); extracellular matrix proteins bind to glycolipids or proteinaceous receptors on cells (Yamada et al., 1985; Roberts, 1987); spectrin, the major component of the erythrocyte cytoskeleton, binds to phosphatidylserines in the inner leaflet of the erythrocyte membrane (Mombers et al., 1980; Maksimiw et al., 1987); many amphiphilic peptides like melittin or signal peptides have a strong affinity for negatively charged phospholipids (Dufourq & Faucon, 1977; Tamm, 1986).

A frequently used model system to study multivalent ligand binding to membranes has been the interaction of antibodies with lipid haptens that were embedded in liposomes (Kinsky & Nicoletti, 1977; Balakrishnan et al., 1982; Luedtke & Karush, 1982; Petrossian & Owicki, 1984). With a monoclonal IgG,[1] this system provides perhaps the most simple case of multivalent large-ligand binding, since the antibodies are bivalent and monodisperse, and the lipid haptens constitute binding sites that are chemically simple and small relative to the antibody. Although the thermodynamics and kinetics of binding have been investigated for many different pairs of antibodies and soluble haptens in much detail [for reviews, see Karush (1978) and Pecht and Lancet (1977)], the binding of antibodies to membranes with multiple binding sites is more difficult to understand theoretically. Traditionally, the binding data have been fit to Langmuir-type adsorption isotherms (or to the corresponding Scatchard plots), and typical apparent binding constants of the order of 10^7–10^9 M^{-1} have been determined with different lipid haptens. However, these binding constants were dependent on many physical properties such as the binding site density, the lipid fluidity, the cholesterol content, and the chemical nature of the hapten lipid linker, apart from the intrinsic "chemical" binding free enthalpy (Balakrishnan et al., 1982; Luedtke & Karush, 1982; Petrossian & Owicki, 1984).

In the present work, the problem of antibody binding to model membranes at different lipid hapten densities is addressed. It is shown that the binding isotherms at all lipid hapten densities, taken individually, can be fit very well to simple Langmuir adsorption isotherms. However, the apparent binding "constants" obtained by this procedure vary by a factor of 300 (!) in the investigated surface concentration range, and the number of lipids covered by each antibody may decrease below physically acceptable values at high lipid hapten densities. In contrast, when a statistical binding model, which takes into account the size and shape of a large ligand on a certain binding site lattice (Stankowski, 1983b), is adapted to the problem of bivalent binding to dilute and mobile binding sites on a membrane, all measured binding curves are easily simulated with a single binding constant and the given lipid hapten density.

Materials and Methods

Lipids and Antibody. DMPC (Fluka, Switzerland) and TNP-cap-eggPE and Rh-DOPE (both from Avanti Polar Lipids) were pure on silica gel thin-layer chromatograms and were used without further purification. The monoclonal anti-TNP IgG (γ_{2b}, κ) was harvested from cultures of the cell line GK14-1, purified, and labeled with fluorescein as described (Tamm, 1988). It had a high binding activity in ELISA tests, and 1.2 mol of fluorescein bound per mole of antibody (Tamm, 1988).

Lipid Vesicles. The appropriate amounts of lipids were mixed from stock solutions in $CHCl_3$. The solvent was re-

† This work was supported, in part, by Swiss National Science Foundation Grant 3.588.87.

[1] Abbreviations: DMPC, 1,2-dimyristoyl-*sn*-3-phosphatidylcholine; IgG, immunoglobulin G; PIPES, piperazine-*N*,*N*′-bis(2-ethanesulfonic acid); Rh-DOPE, *N*-(lissamine rhodamine B sulfonyl)-1,2-dioleoyl-*sn*-3-phosphatidylethanolamine; TNP-cap-eggPE, [[*N*-(2,4,6-trinitrophenyl)amino]caproyl]phosphatidylethanolamine (PE from egg).

0006-2960/88/0427-7453$01.50/0

moved with N_2, and 10 mM PIPES, pH 7.4, containing 0.15 M NaCl was added to give 5 mM total lipid. Small unilamellar vesicles were prepared by 15–20-min tip sonication on a MSE sonicator at 30 °C under argon.

Fluorescence Measurements. The fluorescence measurements were carried out on a Schoeffel RRS 1000 fluorometer. For the binding assays, excitation was at 480 nm and the fluorescence emission was recorded at 513 nm. Slits with bandwidths of 2 and 4 nm were used for excitation and emission, respectively. The amount of antibody bound was measured from the experimental binding parameter, defined as $b = 1 - F/F_0$, where F_0 is the fluorescence intensity before and F the fluorescence intensity after the addition of a given amount of vesicles. Binding at saturation is designated as b_{max}, and the degree of binding is b/b_{max}. The TNP-lipid alone (without Rh-DOPE) did not quench the fluorescein emission efficiently, and hence, corrections due to this effect were unnecessary.

Computer Simulations and Computer Fits. Simulations of the nonspecific and the specific binding models were performed on an Apple IIgs personal computer. The large-ligand binding model was simulated on a VAX 8800 computer by using a numerical procedure based on a binary search technique solving eq 9: Briefly, for each total binding site concentration the degree of binding was estimated, as the mean between two extreme limits, then entered into the binding equation, and compared with the resulting degree of binding. If the estimate was larger/smaller then the calculated value, the upper/lower limit was reset to the estimate and a new mean value was calculated. This procedure converges rapidly ($\sim$10 cycles) to a precision better than 10^{-3}. The computer fits to all binding models were done on the VAX computer by using a least-squares Marquardt routine. The functions were solved either analytically (nonspecific binding) or numerically (specific binding and large-ligand binding).

Results and Discussion

Binding Models. Frequently, ligand binding to a membrane is treated by the simple binding equation

$$KC_A^f = nr/(1 - nr) \quad (1)$$

where r equals the mole fraction of bound ligand to total lipid ($r = C_A^b/C_L^0$), C_A^f is the concentration of free ligand, K is the binding constant, and n is the stoichiometry of binding, i.e., the number of total lipids consumed by each bound ligand at saturation. Thus, an ensemble of n lipids (or subunits, in a more general terminology) is assumed to constitute one ("nonspecific") binding site in this model. Plotting r against C_A^f, eq 1 leads to a hyperbolic adsorption isotherm, which in the case of $n = 1$ is the Langmuir adsorption isotherm. Often eq 1 is also represented in the form of the Scatchard equation

$$r/C_A^f = (K/n)(1 - nr) \quad (2)$$

and a plot of r/C_A^f vs r yields a straight line with the slope $-K$. However, this simple treatment is only correct when the individual binding sites are isolated from each other and do not overlap. In a series of papers (Stankowski, 1983a,b, 1984), Stankowski takes into account the effect of excluded areas on the binding of large ligands to membranes and discusses several different statistical binding models that describe the binding of such ligands to regular lattices of binding sites. It is clear, and has been realized and demonstrated before (Grasberger et al., 1986; Ryan et al., 1988), that large excluded areas in membranes have not only a profound effect on the binding of extrinsic membrane proteins (as discussed here) but can also cause large deviations from ideal behavior for reactions (very large activity coefficients) and redistributions (saturation) of integral membrane proteins in highly crowded cell membranes.

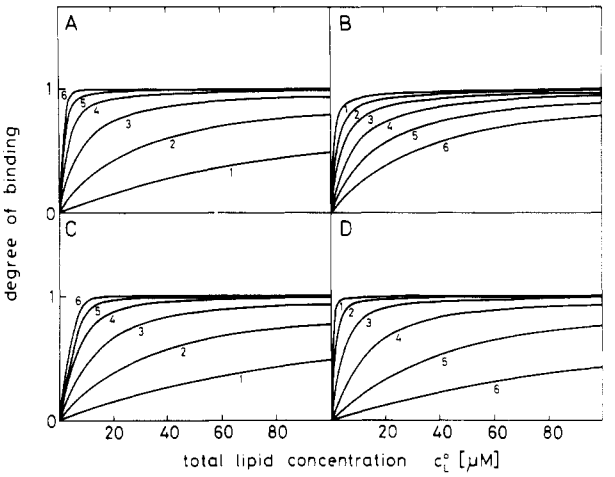

FIGURE 1: Computer simulations of binding isotherms using the nonspecific (eq 1; panels A and B) and the specific (eq 4 with $n = 2m$; panels C and D) binding models. The simulation parameters were as follows: panel A, $n = 100$ (all curves), $K = 1 \times 10^6$, 4×10^6, 1.6×10^7, 6.4×10^7, 2.56×10^8, 1.02×10^9 M^{-1} (curves 1–6); panel B, $K = 1.6 \times 10^7$ M^{-1} (all curves), $n = 12$, 25, 50, 100, 200, 400 (curves 1–6); panel C, $m = 100$ (all curves), $K = 1 \times 10^8$, 4×10^8, 1.6×10^9, 6.4×10^9, 2.56×10^{10}, 1.02×10^{11} M^{-1} (curves 1–6); panel D, $K = 1.6 \times 10^9$ M^{-1} (all curves), $m = 12$, 25, 50, 100, 200, 400 (curves 1–6). The total ligand concentration was 31.3 nM in all simulations.

In this work, we have studied the binding of a bivalent antibody (IgG) to model membranes with different binding site (lipid hapten) densities. In order to understand the experimentally obtained binding isotherms, we first write the law of mass action in its most general form for binding to the surface of a membrane:

$$KC_A^f = r/(X_L)^f \quad (3)$$

$(X_L)^f$ is the mole fraction of free lipid arranged in a geometry suitable for binding an antibody molecule. It remains now to determine $(X_L)^f$ for the different binding models, which in some cases can become a quite formidable task (Stankowski, 1983a,b, 1984; Macdonald & Seelig, 1987). As discussed already, the most simple (and most frequently used) approach is the *nonspecific binding* model, where $(X_L)^f = X_L^f/n$; i.e., the mole fraction of free binding sites equals the mole fraction of free lipid divided by the lipid-to-protein stoichiometry n. This substitution together with the mass conservation equation immediately leads to the binding eq 1. Computer simulations of some typical binding curves using this equation are shown in Figure 1A,B.

Next, in analogy to binding in solution, where two soluble haptens can bind to each antibody, $(X_L)^f = (X_L^f/m)^2$ is considered for bivalent antibody binding to a membrane. In this *specific binding* model, m equals the reciprocal of the mole fraction of lipid hapten, X_{LH}, in the membrane. The appropriate binding equation reads

$$KC_A^f = m^2r/(1 - nr)^2 \quad (4)$$

with $n = 2m$. Considering the large size of the antibody combining site relative to a lipid hapten in a simplistic fashion, one may limit n in the denominator of eq 4 at a minimal value $n_{min} = 86$ (see below) regardless of X_{LH}. Some selected isotherms obeying eq 4 and showing the effect of varying K and m are depicted in Figure 1C,D. As for nonspecific binding, these curves appear to be hyperbolic, but with values of K and n (or m) that are quantitatively very different. The simulations of Figure 1 also show very clearly that virtually identical

binding isotherms can be obtained with both models under appropriate conditions [e.g., cf. curves 5 (1A) and 2 (1D) or curves 6 (1B) and 2 (1C)] and that a distinction between the two models cannot be made by a mere comparison of the fit qualities of the experimental data to one or the other model. A similar conclusion was reached for Ca^{2+} binding to POPC model membranes (Macdonald & Seelig, 1987).

The models described so far neglect excluded area effects due to the large size of the ligand. As mentioned previously, the number of *available* free binding sites on the membrane depends not only on the degree of saturation but also on the size and shape of the bound ligand. For large compact ligands, the simplified Andrews model as suggested by Stankowski seems to be most appropriate. This model was originally conceived as a hard core fluid model (Andrews, 1975, 1976) and later used to describe the binding of large ligands to a regular lattice of equivalent binding sites (Stankowski, 1983b). However, as shown here, this model may be extended to describe the binding of large ligands to mobile binding sites randomly distributed in a fluid (and otherwise nonreactive) membrane. In what follows, we only discuss the large-ligand effect on the bivalent specific binding model, since this seems to be most adequate to describe the binding of IgGs to haptenated model membranes.[2]

The mole fraction of available free sites for the bivalent large ligand is given by the product of three probabilities

$$(X_L)^f = P_1^2 \cdot P_2 \tag{5}$$

P_1 is the probability of finding an unoccupied individual free site:

$$P_1 = X_{LH} \cdot (N - nB)/N = X_{LH} \cdot (1 - nr) \tag{6}$$

where N is the total number of lipids, B is the number of bound ligands (antibodies), and X_{LH}, n, and r have been defined above. If the random distribution of the free binding sites in the membrane is not affected by the binding of the bivalent ligand [an assumption that is strongly supported by lateral diffusion and fluorescence microscope studies on the same antibody and lipid hapten in planar supported bilayers (Tamm, 1988)], then the probability of simultaneously finding two such free binding sites is P_1^2, as has already been stated before for specific binding. Following Andrews and Stankowski, we take P_2, i.e., the probability of finding a free place on the membrane that does not overlap with the excluded area of any of the already bound ligands, as the Bth power of the probability that any one of the B bound molecules is not centered in that area:

$$P_2 = [1 - \alpha u/(N - uB)]^B \tag{7}$$

Here, α is the excluded area parameter, a dimensionless constant that depends on the size and shape of the ligand, and u is the number of lipids covered by each antibody. u equals n only when the total membrane surface can be covered with ligand without gaps, namely, at high binding site densities. The validity of eq 7 implies also that at the lower binding site densities the ligands are allowed to approach each other closely on the membrane surface without significant gaps between the ligands at closest approach. In the limit of large N, eq 7 becomes

$$P_2 = \exp\left(-\frac{\alpha u B}{N - uB}\right) = \exp\left(-\frac{\alpha u r}{1 - ur}\right) \tag{8}$$

[2] We have also fit our data to a nonspecific large-ligand binding model. Although good fits of the individual binding curves were possible, a unique binding constant for *all* lipid hapten densities could not be found.

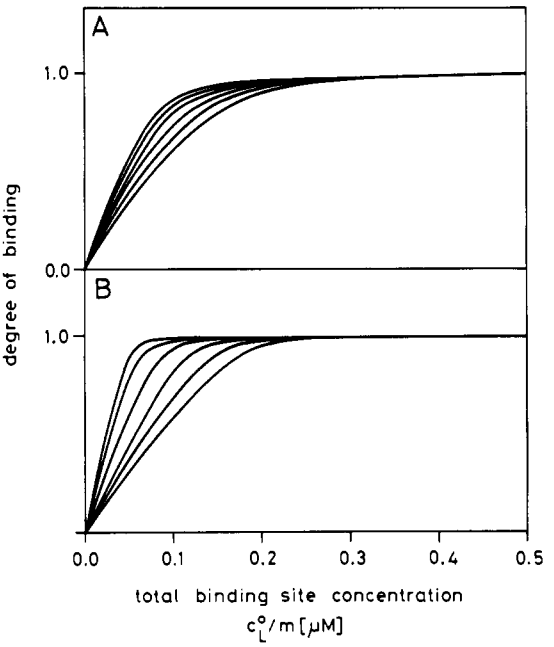

FIGURE 2: Computer simulations of binding isotherms showing the large-ligand effect on the specific binding model (eq 9). The size of the ligand was varied at two different binding site densities, m = 100 and n = 200 (panel A) and m = 10 and n = 86 (panel B), with u = 0, 43, 86, 129, 172, and 215 (curves from left to right in both panels). u is the size (area) of the ligand in terms of the number of lipid subunits covered by each ligand. The binding constant used for all simulations was $K = 3.0 \times 10^{10}$ M^{-1} and the total ligand concentration was 31.3 nM.

Combining eq 3, 5, 6, and 8, we obtain the following *binding* equation for *large bivalent ligands*:

$$KC_A^f = \frac{m^2 r}{(1 - nr)^2} \exp\left(\frac{\alpha u r}{1 - ur}\right) \tag{9}$$

In this model, the lipid-to-protein stoichiometry n equals $2m$ ($=2/X_{LH}$) if $n > u$, or else $n = u$. Equation 9 is similar to eq 26 in Stankowski (1984), which, however, does not incorporate the binding site density ($X_{LH} = 1/m$). Since u and α are constants that can be obtained from the structure of the ligand (see below), K remains as the only free parameter in this model. In order to show the effect of the ligand size on the binding curves, computer simulations with different values of u were carried out for conditions relevant to the case of antibody–lipid hapten binding (Figure 2). Again, the curves look hyperbolic, but are more depressed at high degrees of binding due to the exponential factor in eq 9. As expected, steric hindrance is more pronounced at high binding site densities (Figure 2B), but is still present at densities that do not allow the membrane to be covered completely with ligand ($n > u$ in Figure 2A).

Antibody Binding. Antibody binding to small unilamellar vesicles was measured by monitoring the resonance energy transfer from the fluorescein-labeled antibody to a rhodamine B labeled phospholipid, which served as an efficient energy acceptor when included into the membrane at 5 mol %. Förster theory adapted to the problem of a discrete energy donor at some distance away from an energy-accepting continuous plane predicts that only donors within a shell of ~50 Å from the accepting plane can contribute significantly to the energy-transfer signal (Shaklai et al., 1977). Considering the molecular dimensions of an antibody, fluorescence energy transfer therefore provides an excellent signal to discriminate between bound and unbound antibody. In our experiments, small unilamellar vesicles consisting of DMPC, TNP-cap-

Table I: Summary of Least-Squares Fits to the Nonspecific Binding Model (Equation 1)

lipid hapten in membrane (mol %)	no. of expt	K_{app} (M^{-1})	n^a	area/antibody (nm^2)[b]	no. of lipid haptens per antibody[c]
0.1	1	1.8×10^7	2000[d]	1400	2
0.2	1	4.5×10^7	1000[d]	700	2
0.5	2	$(6.4 \pm 2.2) \times 10^7$	300 ± 120	210	1.5
1.0	2	$(1.4 \pm 0.1) \times 10^8$	190 ± 40	133	1.9
2.0	3	$(5.4 \pm 1.9) \times 10^8$	180 ± 50	126	3.6
3.0	2	$(2.0 \pm 0.5) \times 10^9$	240 ± 10	168	7.2
5.0	2	$(1.2 \pm 0.1) \times 10^9$	200 ± 50	140	10
10.0	3	$(5.4 \pm 1.4) \times 10^9$	120 ± 20	84	12

[a] Total lipid to bound antibody ratio at saturation. [b] Area per bound antibody at saturation (lipid area = 0.70 nm^2). [c] Lipid hapten to bound antibody ratio at saturation. [d] Taken as a constant, i.e., not a free fit parameter.

eggPE, and Rh-DOPE were titrated to a fixed amount of fluorescent antibody kept at 25 °C, and the binding parameter was determined as described under Materials and Methods.

Selected binding curves, obtained at increasing lipid hapten densities in the vesicles, are shown in Figure 3. Note that, in order to obtain curved isotherms, the total antibody concentration in the cuvette also had to be changed when binding became stronger at high lipid hapten densities. Parallel experiments were run with vesicles without lipid hapten or with an irrelevant antibody. Both showed no binding, and only a small increase in resonance energy transfer due to random collisional quenching was observed at high total lipid concentrations (not shown). Our data are not corrected for this effect. Also, we did not observe any significant amount of vesicle cross-linking by the antibody under the employed experimental conditions. This finding is in agreement with theoretical results of Crothers and Metzger (1972), who emphasized that multisite adherence to single particles predominates strongly over cross-linking of discrete particles as long as the receptor density on the particle is not extremely low. Petrossian and Owicki (1984) also found mainly "monogamous" binding of antibodies to haptenated membranes, whereas Luedtke and Karush (1982) observed "heterogamous" binding and lipid precipitation in a related system. The origin of this discrepancy is unknown at present.

The aim of this work was to find an accurate description of the binding mechanism of bivalent IgG to lipid model membranes. It has been shown in the previous section that completely different binding models can lead to virtually superimposable binding curves. Therefore, individual fits to the experimental data are *not* sufficient to discriminate between the different models. Additional information is required, and this can be obtained from a comparison of the fit parameters at the different lipid hapten densities. In the following, we discuss the same experimental data in terms of the three binding models that have been introduced above.

The binding data were first fit by a nonlinear Marquardt procedure to the *nonspecific binding* model of eq 1. The two free fit parameters K and n were evaluated for each curve, and the best fits are shown as solid lines in Figure 3. (The end value, b_{max}, was taken directly from the data where appropriate, or adapted manually within a narrow range when saturation was not achieved.) The best fit values together with the results of more binding curves are summarized in Table I. According to the nonspecific binding model, the apparent binding constants are found to increase over more than 2 orders of magnitude between 0.1 and 10 mol % lipid hapten, and the area on the membrane per bound antibody levels off at rather large values at high lipid hapten densities (cf. below). Thus, even though the individual fits with the nonspecific binding model are very good (Figure 3), this model is unable to provide a unique binding constant independent of the lipid hapten concentration in the membrane.

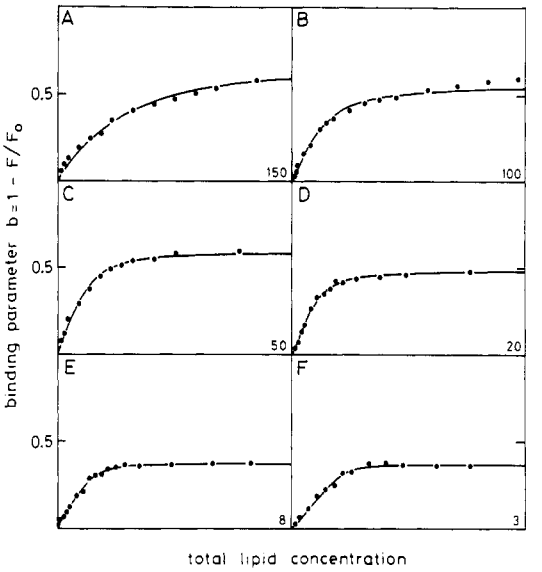

FIGURE 3: Antibody binding to DMPC vesicles containing the lipid hapten TNP-cap-eggPE at various mole percentages: 0.2 (panel A), 0.5 (panel B), 1.0 (panel C), 2.0 (panel D), 3.0 (panel E), and 10.0 (panel F). Binding of the fluorescein-labeled antibodies was measured by recording the resonance energy transfer to the rhodamine B labeled vesicles. The total antibody concentrations were 31.3 (panels A–C), 10.2 (panel D), and 5.0 nM (panels E and F). The total widths of the abscissas are indicated (in μM) in the lower right corner of each panel. The curves show the best computer fits using the *nonspecific binding model* (eq 1). The best fit parameters were as follows (see also Table I): $K = 4.5 \times 10^7$ M^{-1}, $n = 1000$ (panel A); $K = 7.9 \times 10^7$ M^{-1}, $n = 387$ (panel B); $K = 1.4 \times 10^8$ M^{-1}, $n = 212$ (panel C); $K = 7.6 \times 10^8$ M^{-1}, $n = 244$ (panel D); $K = 2.4 \times 10^9$ M^{-1}, $n = 246$ (panel E); $K = 5.9 \times 10^9$ M^{-1}, $n = 134$ (panel F).

Fits of comparable quality as those shown in Figure 3 were obtained with the *specific binding* model (eq 4, figure not shown). In this case, the binding constant K was the only free fit parameter and m was kept constant at $m = 1/X_{LH}$. A summary of the best fit parameters of 18 binding curves is given in Table II. A comparison of the listed binding constants shows that a substantial improvement over the nonspecific binding model has already been achieved and that up to 1 mol % lipid hapten a single apparent binding constant of $\sim 2 \times 10^{10}$ M^{-1} could be assigned. However, at larger lipid hapten densities, this model (with a limited or an unlimited stoichiometry n) breaks down too, and large-ligand effects must be included. The improvement over the nonspecific model at low lipid hapten densities is even more striking if one recalls that the number of free fit parameters has been reduced from two to one.

In order to apply the *large-ligand binding* model (eq 9), information on the molecular dimensions of the IgG molecule is required. For this analysis, we assume that each bound

Table II: Summary of Least-Squares Fits to the Specific Binding Model (Equation 4)

lipid hapten in membrane (mol %)	no. of expt	unlimited model $10^{-10}K_{app}$ (M^{-1})	unlimited model $n = 2m^a$	limited model $10^{-10}K_{app}$ (M^{-1})	limited model n^b
0.1	1	1.76	2000		
0.2	1	1.81	1000		
0.5	2	2.00 ± 0.78	400		
1.0	3	2.56 ± 1.27	200		
2.0	4	0.78 ± 0.35	100		
3.0	2	0.18 ± 0.08	66.7	0.24 ± 0.09	86
5.0	2	0.070 ± 0.047	40	0.14 ± 0.11	86
10.0	3	0.038 ± 0.002	20	0.36 ± 0.20	86

[a] Unlimited model: lipid to bound antibody ratio at saturation is taken to be fixed at twice the lipid to lipid hapten ratio. [b] Limited model: at high lipid hapten densities the lipid-to-protein ratio at saturation is 86, i.e., the number of lipids covered by one antibody (see text).

antibody covers a rectangular area of 5 × 12 nm^2 on the surface of the membrane. This rectangle is taken to be slightly more compact than the rectangle calculated from the known antibody crystal structures (4–5 × 14–15 nm; Coleman et al., 1976; Sarma et al., 1971), because the antibody molecule is known to be flexible in the hinge region (Feinstein & Rowe, 1965; Valentine & Green, 1967; Yguerabide et al., 1970) and the hinge angle is expected to be somewhat smaller for an antibody bound to the membrane by both combining sites as compared to a free antibody. Since phospholipids have a cross section of ~0.70 nm^2, each antibody covers $u = 86$ lipids. Following the rules given by Stankowski (1983b), we calculated an excluded area parameter $\alpha = 2.95$ for the 5 × 12 nm^2 antibody–membrane interface. It should be noted that α is rather insensitive to small changes in shape as long as the interface area is large (compared to a phospholipid) and its shape is relatively compact. For instance, if this area was a circle or a regular hexagon of the same size, α would be 3.0 or 2.63, respectively.[3]

Having determined u and α, the experimental data can now be fit to eq 9 with K being the *only* free fit parameter. The best fits to selected binding curves at various lipid hapten densities are shown in Figure 4, and a summary of all performed fits is given in Table III. Except for the binding constants at 10 mol % (which are somewhat too high), the agreement between the binding constants of all experiments over a wide range of lipid hapten densities is remarkable. If these are all averaged, we find a *unique binding constant* $K = (2.8 \pm 1.4) \times 10^{10}$ M^{-1} for the binding of the monoclonal mouse immunoglobulin GK14-1 to TNP-lipid haptens in DMPC model membranes at 25 °C.

In summary, the work presented here strongly supports earlier theoretical concepts on the binding of large ligands to membranes and shows that excluded areas have to be invoked to describe the binding of immunoglobulins to haptenated model membranes correctly. Obviously, the large-ligand effect becomes most pronounced at high lipid hapten densities (>2 mol %). Nevertheless, it still causes significant perturbations of the binding isotherms at intermediate binding site concentrations (0.2–1 mol %). As a consequence of this and due to the fact that bivalency was neglected in earlier studies of antibody–lipid hapten binding (Balakrishnan et al., 1982; Luedtke & Karush, 1982; Petrossian & Owicki, 1984), the binding constants were underestimated by these authors. The free enthalpy change of binding found here for bivalent binding, approximately −14.5 kcal/mol, is somewhat smaller than twice the free enthalpy change for monovalent hapten binding in solution (typically −10 to −12 kcal/mol). This is not surprising, since the accessibility of a lipid hapten is limited by the membrane. It is expected, therefore, that longer and more hydrophilic chemical linkers between the phosphorus and hapten moieties of the lipid hapten will increase the antibody affinity for haptenated membranes (Balakrishnan et al., 1982).

[3] The model leading to eq 9 was originally derived only for large ligands that are fully symmetric. However, it has been shown that eq 9 describes the binding of nonsymmetrically shaped ligands too, as long as the ligand covers more than ~10 lipids (Stankowski, 1984).

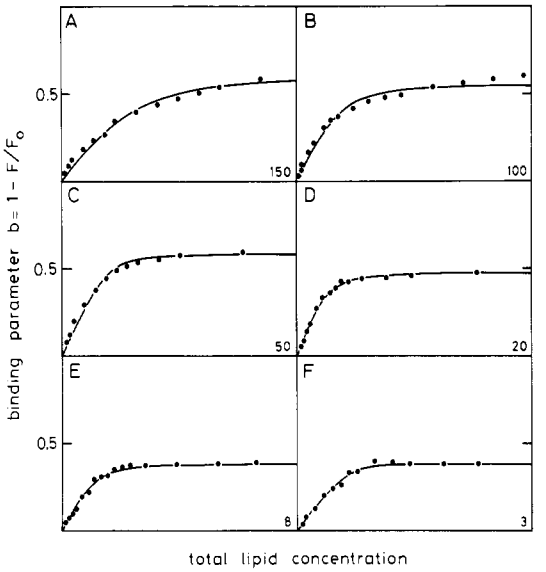

FIGURE 4: Antibody binding to DMPC vesicles containing the lipid hapten TNP-cap-eggPE at various mole percentages. The same experimental data are displayed as in Figure 3 (see legend to Figure 3 for experimental details). The curves show the best computer fits using the *bivalent large-ligand binding model* (eq 9). The best fit parameters were as follows (see also Table III): $K = 3.47 \times 10^{10}$ M^{-1} (panel A), $K = 2.51 \times 10^{10}$ M^{-1} (panel B), $K = 3.69 \times 10^{10}$ M^{-1} (panel C), $K = 1.19 \times 10^{10}$ M^{-1} (panel D), $K = 1.47 \times 10^{10}$ M^{-1} (panel E), $K = 1.45 \times 10^{11}$ M^{-1} (panel F). All other parameters were fixed as described in the text: $m = 1/X_{LH}$, $u = 86$, $n = 2m$ if $m > 43$ or $n = 86$ if $m \leq 43$.

Table III: Summary of Least-Squares Fits to the Large-Ligand Binding Model (Equation 9)

lipid hapten in membrane (mol %)	total antibody concn (nM)	$10^{-10}K$ (M^{-1})	$10^{-10}K_{av}$ (M^{-1})	n^a	m^b
0.1	31.3	2.36		2000	1000
0.2	31.3	3.47		1000	500
0.5	31.3	2.51	3.30 ± 1.11	400	200
	31.3	4.08		400	200
1.0	31.3	3.69		200	100
	31.3	4.00	3.73 ± 0.25	200	100
	31.3	3.50		200	100
2.0	10.2	3.13		100	50
	10.2	5.78	3.37 ± 2.30	100	50
	10.2	1.19		100	50
3.0	10.2	1.02	1.25 ± 0.32	86	33.3
	5.0	1.47		86	33.3
5.0	10.2	1.52		86	20
	5.0	3.60	1.93 ± 1.50	86	20
	5.0	0.68		86	20
10.0	5.0	14.5	20.7 ± 8.7	86	10
	5.0	28.8		86	10
K		2.80 ± 1.42[c]	2.72 ± 1.07[d]		

[a] Total lipid to bound antibody ratio at saturation. [b] Total lipid to lipid hapten ratio. [c] Average of all individual binding constants, 10 mol % excluded. [d] Average of all averaged binding constants, 10 mol % excluded.

ACKNOWLEDGMENTS

We acknowledge Prof. G. Köhler for his kind gift of the hybridoma cell line GK14-1. We thank Dr. H. Christen for his help with the numerical fit programs, Dr. S. Stankowski for fruitful discussions and critically reading the manuscript, and E. Johner for typing the manuscript.

REFERENCES

Alving, C. R. (1984) *Biochem. Soc. Trans. 12*, 342-344.
Andrews, F. C. (1975) *J. Chem. Phys. 62*, 272-275.
Andrews, F. C. (1976) *J. Chem. Phys. 64*, 1941-1947.
Balakrishnan, K., Mehdi, S. Q., & McConnell, H. M. (1982) *J. Biol. Chem. 257*, 6434-6439.
Coleman, P. M., Deisenhofer, J., & Huber, R. (1976) *J. Mol. Biol. 100*, 257-282.
Crothers, D. M., & Metzger, H. (1972) *Immunochemistry 9*, 341-357.
Dufourcq, J., & Faucon, J. L. (1977) *Biochim. Biophys. Acta 467*, 1-11.
Feinstein, A., & Rowe, A. J. (1965) *Nature (London) 205*, 147-149.
Grasberger, B., Minton, A. P., DeLisi, C., & Metzger, H. (1986) *Proc. Natl. Acad. Sci. U.S.A. 83*, 6258-6262.
Karush, F. (1978) *Compr. Immunol. 5*, 85-116.
Kinsky, S. C., & Nicoletti, R. A. (1977) *Annu. Rev. Biochem. 46*, 49-67.
Luedtke, R., & Karush, F. (1982) *Biochemistry 21*, 5738-5744.
Macdonald, P. M., & Seelig, J. (1987) *Biochemistry 26*, 1231-1240.
Maksimiw, R., Sui, S., Gaub, H., & Sackmann, E. (1987) *Biochemistry 26*, 2983-2990.
Mombers, C., de Gier, J., Demel, R. A., & van Deenen, L. L. M. (1980) *Biochim. Biophys. Acta 603*, 52-62.
Pangborn, M. C. (1942) *J. Biol. Chem. 143*, 247-256.
Pecht, I., & Lancet, D. (1977) in *Chemical Relaxation in Molecular Biology* (Pecht, I., & Rigler, R., Eds.) pp 306-338, Springer, New York.
Peitsch, M. C., Kovacsovics, T. J., Tschopp, J., & Isliker, H. (1987) *J. Immunol. 138*, 1871-1876.
Petrossian, A., & Owicki, J. C. (1984) *Biochim. Biophys. Acta 776*, 217-227.
Roberts, D. D. (1987) *Methods Enzymol. 138*, 473-483.
Ryan, T. A., Myers, J., Holowka, D., Baird, B., & Webb, W. W. (1988) *Science (Washington, D.C.) 239*, 61-64.
Sarma, V. R., Silverton, E. W., Davies, D. R., & Terry, W. D. (1971) *J. Biol. Chem. 246*, 3753-3759.
Schumaker, V. N., Zavodszky, P., & Poon, P. H. (1987) *Annu. Rev. Immunol. 5*, 21-42.
Shaklai, N., Yguerabide, J., & Ranney, H. M. (1977) *Biochemistry 16*, 5585-5592.
Stankowski, S. (1983a) *Biochim. Biophys. Acta 735*, 341-351.
Stankowski, S. (1983b) *Biochim. Biophys. Acta 735*, 352-360.
Stankowski, S. (1984) *Biochim. Biophys. Acta 777*, 167-182.
Tamm, L. K. (1986) *Biochemistry 25*, 7470-7476.
Tamm, L. K. (1988) *Biochemistry 27*, 1450-1457.
Valentine, R. C., & Green, N. M. (1967) *J. Mol. Biol. 27*, 615-617.
Yamada, K. M., Akiyama, S. K., Hasegawa, T., Hasegawa, E., Humphries, M. J., Kennedy, D. W., Nagata, K., Urushihara, H., Olden, K., & Chew, W.-T. (1985) *J. Cell. Biochem. 28*, 79-97.
Yguerabide, J., Epstein, H. F., & Stryer, L. (1970) *J. Mol. Biol. 51*, 573-590.

Characterization of the Enzymatic Conversion of Sulfoacetaldehyde and L-Cysteine into Coenzyme M (2-Mercaptoethanesulfonic Acid)†

Robert H. White

Department of Biochemistry and Nutrition, Virginia Polytechnic Institute and State University, Blacksburg, Virginia 24061

Received April 8, 1988; Revised Manuscript Received June 2, 1988

ABSTRACT: Sulfoacetaldehyde was shown to be converted enzymatically into coenzyme M by cell-free extracts of methanogenic bacteria. Gas chromatography–mass spectrometry (GC–MS) of the *S*-methyl methyl ester derivative of the coenzyme M isolated from the extracts was used to measure both the extent and position of the deuterium incorporated into coenzyme M from [2,2-$^2H_2$]sulfoacetaldehyde. The conversion of sulfoacetaldehyde into coenzyme M was greatly stimulated by the addition of L-cysteine (20 mM) to the extracts and/or by incubating the extracts under hydrogen, whereas incubation in the presence of sulfide (20 mM) greatly reduced coenzyme M synthesis. Incubation of a cell-free extract from *Methanobacterium formicicum* with [2,2-$^2H_2$]sulfoacetaldehyde and [^{34}S]-L-cysteine (92.6 atom % ^{34}S) led to the production of coenzyme M in which the thiol portion of the molecule contained 90 atom % ^{34}S. [*ethylene*-$^2H_4$]-*S*-(2-Sulfoethyl)cysteine, incubated with this cell-free extract at a concentration of 22 mM, readily cleaved to coenzyme M. On the basis of these observations, it is concluded that sulfoacetaldehyde is converted into coenzyme M by reacting with cysteine to form the thiazolidine adduct [2-(sulfomethyl)thiazolidine-4-carboxylic acid], which undergoes a reductive cleavage of the heterocyclic C(2)–N bond to form *S*-(2-sulfoethyl)cysteine, which, in turn, undergoes a β-elimination to produce coenzyme M.

Coenzyme M (2-mercaptoethanesulfonic acid) is one of several recently described coenzymes involved in the biological production of methane (Escalante-Semerena et al., 1984). The methylation of coenzyme M to *S*-methyl-coenzyme M, which undergoes a subsequent reductive cleavage to methane and coenzyme M, is involved in the production of methane from H_2 and CO_2 (Escalante-Semerena et al., 1984), methanol and

†This work was funded by National Science Foundation Grant PCM-8217072.

0006-2960/88/0427-7458$01.50/0